SPACE TELESCOPE SCIENCE INSTITUTE
Operated for NASA by AURA

Instrument Science Report STIS 2006-01

Charge Transfer Efficiency of the STIS CCD:
The time dependence of charge loss and centroid shifts from Internal Sparse Field data

Paul Goudfrooij, Jesús Maíz-Apellániz, Tom Brown, & Randy Kimble
February 27, 2006

ABSTRACT

We describe the Internal Sparse Field test used to characterize relevant aspects of the decreasing Charge Transfer Efficiency (CTE) of the STIS CCD with elapsed on-orbit time. We measure two main observational effects of CTE: Fractional signal loss and centroid shift, using artificial point-source spectra read out by amplifiers at both serial registers. We derive time constants of the increases of fractional signal loss (21.8% yr^{-1}) and centroid shift (16.0% yr^{-1}) due to CTE effects, and find a very tight relation between the two. This relation should be useful for science programs requiring sub-pixel astrometric accuracy. Finally, we compare results in the two supported gain settings of the STIS CCD (gain = 1 and gain = 4).

1 Introduction

The high flux of damaging radiation at the altitude of the HST orbit produces a continuously increasing population of charge traps in the silicon of Charge-Coupled Devices (CCDs) which decreases the latter's charge transfer efficiency (CTE), which is quantified by the fraction of charge successfully moved (clocked) between adjacent pixels. In practice it is often more useful to use the term Charge Transfer *Inefficiency* (CTI $\equiv 1-$CTE). The main observational effect of CTI is that a star whose induced charge has to traverse many pixels before being read out appears to be fainter than the same star observed near the read-out amplifier. The effect is significant for all CCD detectors used on *HST* instruments (e.g., Whitmore et al. 1999; Goudfrooij & Kimble 2003; Riess & Mack 2004). Several aspects of on-orbit characterizations of the CTI of the STIS CCD have been

reported by Gilliland, Goudfrooij, & Kimble (1999), Kimble, Goudfrooij, & Gilliland (2000), Goudfrooij & Kimble (2003), and Bohlin & Goudfrooij (2003). Here we report on a rather unique and sensitive test of CTI, designated the "internal sparse field" test. This is the only CTI test that has been conducted with the STIS CCD in a uniform manner, both during ground testing and during in-flight operation of STIS on an annual basis. It is therefore perhaps no surprise that it yields the most robust determination of the time dependence of the CTI of the STIS CCD, which has been used as such for CTI corrections in the 1-D spectral extraction step in the CALSTIS pipeline (for spectroscopic observations) since 2003. This report has two main purposes: *(i)* it describes the determination of the time constant of CTI increase from all internal sparse field measurements obtained during the lifetime of STIS, and *(ii)* it provides a quantitative measure of the centroid shifts caused by CTI effects as a function of time and signal level.

2 Internal Sparse Field Test

This test method quantifies two key aspects of CTE effects on spectroscopic measurements: *(i)* The amount of charge lost *outside* a standard extraction aperture, and *(ii)* the amount of centroid shift experienced by the charge remaining *within* that extraction aperture. The test utilizes the ability of the STIS CCD and its associated electronics to read out the image with any amplifier, i.e., by clocking the accumulated charge in either direction along both parallel and serial registers. A sequence of nominally identical exposures is taken, alternating the readout between amplifiers on either side of the CCD (e.g., amps 'B' and 'D' for measuring parallel CTI performance[1]). After correcting for (small) gain differences in the two readout amplifier chains, the observed ratio of the fluxes measured by the two amps can be fit to a simple CTI model of constant fractional charge loss per pixel transfer (i.e., per row for parallel CTI measurements). Inspecting the dependence of the observed flux ratio (e.g., 'amp B'/'amp D') on the source position on the CCD, it can be confirmed that what is measured is indeed consistent with being due to a charge transfer effect (cf. Fig. 2 below).

A key virtue of this method is that neither a correction for flat-field response non-uniformity is required, nor an a-priori knowledge of the source flux (as long as the input source is stable during the alternating exposures). It should be noted that what is being measured is actually a sum of the charge transfer inefficiencies for the two different clocking directions. However, for identical clocking voltages and waveforms and with the expected symmetry of the radiation damage effects, we believe the assumption that the CTI is equal in the two different directions is a reasonable one.

The implementation of this "internal"[2] version of the sparse field test is as follows. Using an onboard tungsten lamp, the image of a narrow slit which runs along the dipersion direction[3] is projected at five positions along the CCD columns. At each position, a sequence of exposures is taken, alternating between the 'B' and 'D' amplifiers for readout. An illustration of such an exposure sequence is depicted in Fig. 1. The exposure setup used for these observations is listed in Table 1, while the calibration program numbers and dates of each observing epoch are given in Table 2.

The illumination of these images is representative for typical spectroscopic observations (as the dispersion direction of STIS CCD spectral modes is essentially along rows). The slit image has a narrow profile (2-pixel FWHM), similar to a point source spectrum. The CTI resulting from this test is "worst-case", since

[1]The CTI of the STIS CCD is only significant in the parallel readout direction (e.g., Kimble et al. 2000). Hence, the remainder of this report only addresses *parallel* CTI.

[2]"internal" in this context means that all necessary observations are using onboard lamps, so that such observations can be performed during Earth occultations, hence not requiring any valuable "external" *HST* observing time.

[3]We note that such slits are "special" apertures meant for calibration purposes; their orientation is perpendicular to the slits used for 'normal' STIS spectra

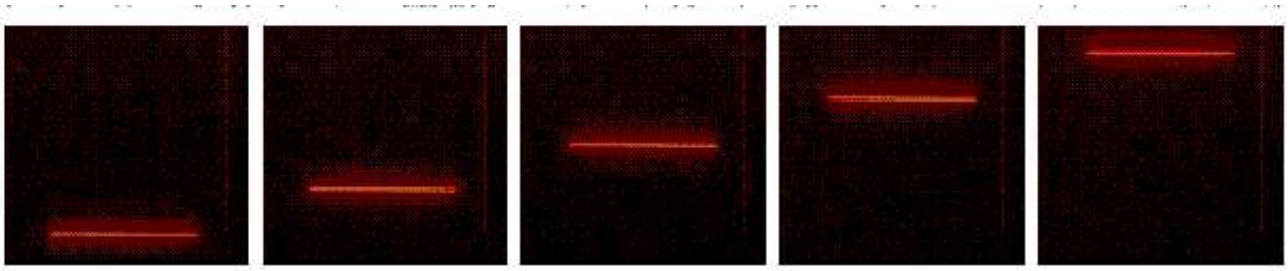

Figure 1: Representative images used for the "internal" sparse field CTE test in the parallel clocking direction. At each of the five positions along the CCD columns, a sequence of exposures is taken, alternating between amplifiers 'B' and 'D' on either side of the parallel register. Systematic variation of the relative signals measured by the two amplifiers as a function of position reveals the CTE effects. A logarithmic stretch is used for display.

Table 1: Setup of STIS observations for "internal" sparse field tests.

Optical Element	$\lambda_{\rm cen}$ (Å)	Slit Name	Exp. Time (s)	CCD Gain (e^-/DN)	Signal Level[a]
G430M	5471	0.05x31NDA	0.3	1, 4	60
G430M	5471	0.05x31NDA	0.6	1, 4	130
G430M	5471	0.05x31NDA	0.9	1, 4	195
G430M	5471	0.05x31NDA	2.3	1, 4	500
Mirror	—[b]	0.05x31NDA	0.3	1, 4	3450
Mirror	—[b]	0.05x31NDB	0.3	1, 4	9850

[a] Unit is e^- per column *in the absence of CTE losses*.
[b] Using 'Clear' filter (i.e., no filter; aperture name 50CCD)
Notes: All exposures were taken in two read modes: Once read out using the default amplifier 'D', and once using amplifier 'B' on the opposite side of the parallel register.

Table 2: Observing blocks used in this work. Each block extended over a time period of one to a few days. Representative values for the Modified Julian Date (MJD) and the civil date are shown.

Gain	Block	Program	MJD	Date (UT)
1	1	8414	51428	Sep 07, 1999
1	2	8414	51650	Apr 16, 2000
1	3	8851	51845	Oct 28, 2000
1	4	8910	52210	Oct 28, 2001
1	5	9620	52567	Oct 20, 2002
1	6	9620	52896	Sep 14, 2003
4	1	8414	51783	Aug 26, 2000
4	2	8851	52004	Apr 04, 2001
4	3	8910	52399	May 05, 2002
4	4	9620	52734	Apr 05, 2003
4	5	10026	53099	Apr 04, 2004

there is rather little background intensity ("sky") to provide filling of charge traps in the CCD silicon lattice.

For each exposure, the average flux per column integrated over a 7-row extraction aperture (which is the default extraction size for long slit STIS spectra of point sources, cf. Leitherer & Bohlin 1997; McGrath et al. 1999) as well as the centroid of the image profile within those 7 rows are calculated. A measurement of the background level was obtained 40 pixels above and below the extracted flux with a width of 5 rows to reflect the flux measurement mode used by the 1-d spectral extraction module of the CALSTIS pipeline. Fluxes and backgrounds were clipped in order to reject residual cosmic rays and hot pixels. The alternating exposure sequence allows one to separate CTI effects from flux variations produced by warmup of the internal tungsten lamp. As the slit image extends across hundreds of columns, high statistical precision on CTI performance can be obtained even at low signal levels per column.

We emphasize that in calculating CTI from this test, charge is only considered "lost" if it is no longer within the standard 7-row extraction aperture. I.e., we are only measuring the component of CTI produced by relatively long-time-constant charge trapping. Hence, the CTI values derived from this test will not agree with those measured by (e.g.) X-ray stimulation techniques using Fe^{55} or Cd^{109}, for which charge deferred to even the very first trailing pixel formally contributes to the CTI. However, the measurement described here *is* directly relevant to the estimation of CTE effects on STIS spectrophotometry.

3 Results

A χ^2-minimization algorithm was used to compute CTI for each observing epoch and signal level. After correcting for (small) gain differences in the two readout amplifier chains, the observed ratio of the fluxes measured by the two amplifiers was fit to a simple CTE model of constant fractional charge loss per pixel transfer, allowing for $\kappa - \sigma$ clipping of outliers (the latter arise occasionally from lamp intensity fluctuations of the short (0.3 sec) exposures).

As the results show significant differences between the two supported CCD gain settings, the remainder of this section will be split into two subsections, one for each gain setting. For various reasons which will be clarified below, the results of the gain = 1 e^-/DN setting should be regarded as most relevant.

3.1 Gain = 1

3.1.1 Time dependence of CTE degradation

Flux ratio results for the parallel internal sparse field test taken in gain = 1 after 5.5 years in orbit are presented in Figure 2. It can be seen that a simple CTI model (constant fractional charge loss per pixel transfer) fits the data quite well.

To derive the time dependence of the CTI, all CTI measurements were first normalized to zero background. In order to arrive at that value, two corrections were required: First, the effect of the spurious charge in the STIS CCD bias frames (Goudfrooij & Walsh 1997) was accounted for by considering the total background (B') to be the measured one (B) plus the spurious charge. Second, the previously derived background dependency of the CTI was taken into account:

$$\mathrm{CTI}\,(B', G) = \mathrm{CTI}_0\ \exp\left(-2.97\left(\frac{B'}{G}\right)^{0.21}\right) \tag{1}$$

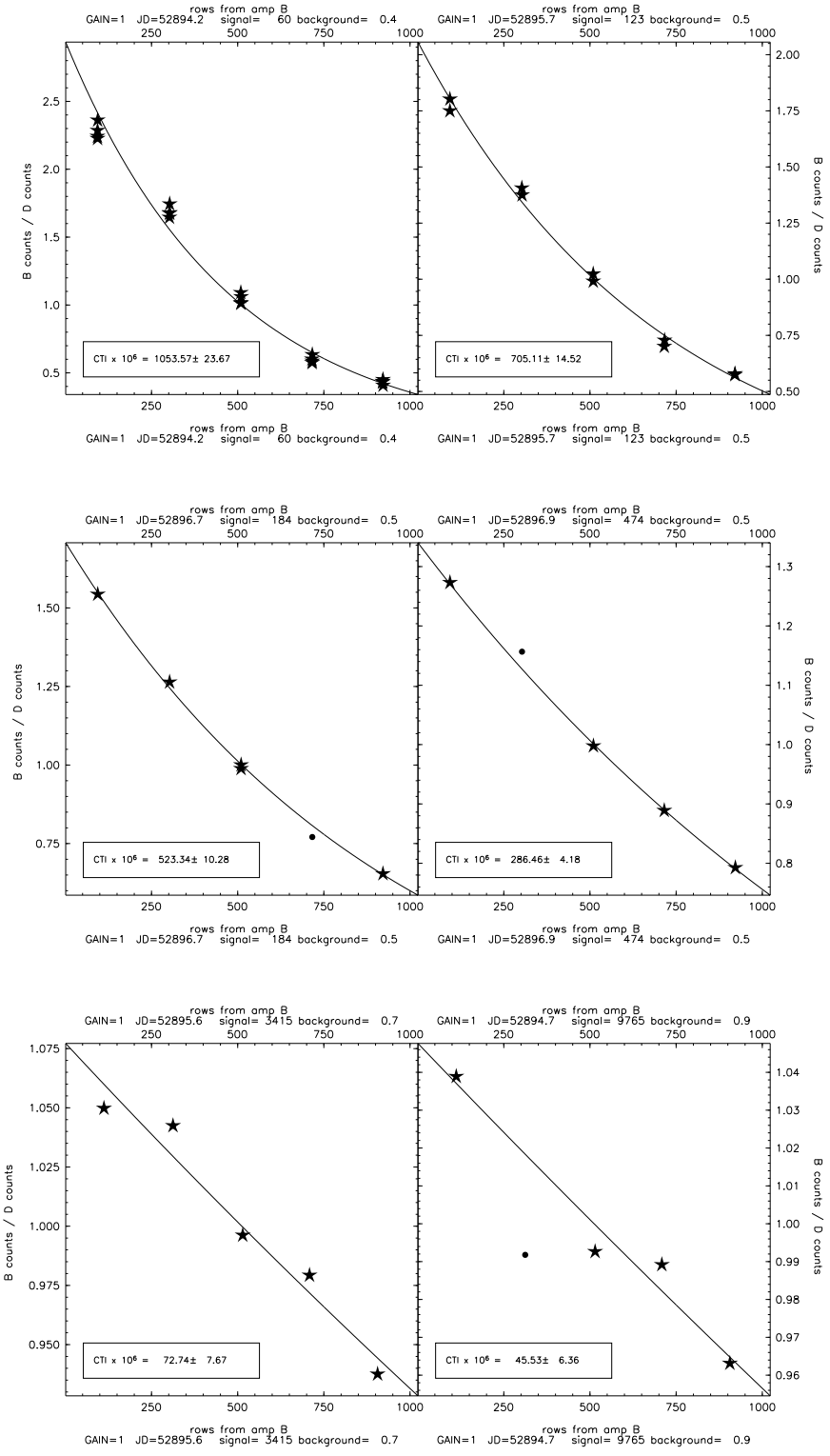

Figure 2: CTI calculation for one of the gain = 1 observing blocks. Each panel shows the data and the fit for a given signal level (which are labelled above and below each panel). Star symbols indicate measurements used in the fit and circles indicate rejected points. Fitted CTI values are indicated in the boxed legend.

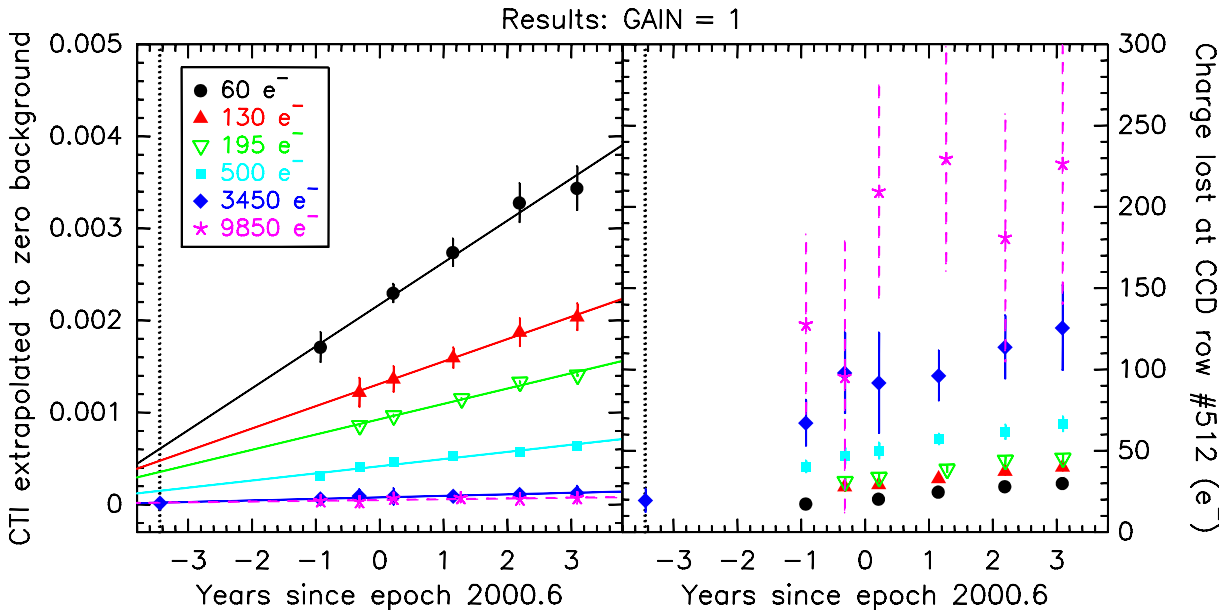

Figure 3: *Left panel:* CTI extrapolated to zero background for gain = 1 as a function of time and signal level, derived from the internal sparse field test. Both the data and the corresponding linear fits are plotted. Symbols associated with individual signal levels (corrected for CTI) are indicated in the legend. *Right panel:* Absolute charge lost due to CTI for an object at the central row of the STIS CCD as a function of time and signal level. Symbol types are the same as in the left panel. The epoch of HST Servicing Mission 2 (during which STIS was installed on HST) is depicted as a black dotted line.

(Bohlin & Goudfrooij 2003)[4] where B' is the total background value and G is the measured gross signal level. The time dependence was derived by fitting the zero-background CTI values to a function of the form:

$$\mathrm{CTI}\,(t) = \mathrm{CTI}_0\,[1 + \alpha(t - t_0)], \tag{2}$$

with t in years and $t_0 = 2000.6$, the approximate midpoint in time of in-flight STIS observations. The conversion between $(t - t_0)$ and the modified Julian date MJD (which is provided by keywords `TEXPSTRT` and `TEXPEND` in the science header of each STIS observation) is given by $t - t_0 = (\mathrm{MJD} - 51765)/365.25$.

CTI values derived as mentioned above for the parallel internal sparse field test taken at different epochs are plotted in Figure 3. In-flight CTE degradation from a pre-flight starting point of low CTI is apparent. Typical CTE-like behavior is observed as a function of signal level: The *fractional* charge loss (which is proportional to CTI) drops with increasing signal level, while the *absolute* level of charge loss increases.

Results for the time-dependence fit for gain = 1 are shown in Fig. 3 and Table 3. The functional fit to the data is quite good, and the derived values for α in Eq. (2) are consistent with one another (within the uncertainties) for all signal levels measured. As to the final selection of the time constant α, we considered that the dataset with 3450 electrons per column is the only one for which pre-flight measurements were available, i.e., it covers a time interval considerably longer than for the other signal levels. Hence $\alpha = 0.218 \pm 0.038$ was selected as representative for all signal levels, as indicated in Table 3.

[4] An updated background dependence of the CTI was recently derived (Goudfrooij et al. 2006, proceedings of 2005 HST Calibration Workshop) and being implemented within the CALSTIS pipeline. However, the differences are negligible for the data considered here.

Table 3: CTE degradation time constant α as a function of signal level for gain = 1. The last row lists our adopted value in boldface font.

signal (DN)	α (yr^{-1})	σ_α (yr^{-1})
60	0.216	0.009
130	0.192	0.013
195	0.188	0.011
500	0.202	0.006
3450	0.218	0.038
9850	0.170	0.052
α = **0.218 $\pm$ 0.038**		

3.1.2 Centroid shift and its dependence on flux loss due to CTI

The effects of charge trapping and release *within* the 7-row aperture are seen by examining the line profiles and centroids. Comparisons of the average line profiles seen for the opposing readout directions are shown in Figure 4 for two of the signal levels used. At 60 electrons per column, the charge trailing and centroid shift are obvious. Even at the higher signal level, with much lower CTI, the magnified difference between the two observed profiles shows that the centroid shift is systematic and measurable. The measured centroid shifts (defined as half the difference between the profile centroids as measured by the two different amplifiers) after 5.5 years in orbit are plotted in the left panel of Figure 5, along with a least-square fit to the centroid shifts measured at the central position on the CCD as a function of measured gross signal level G as read out by the default amplifier D. The fit represents the following function:

$$\log\left(\text{Centroid Shift [pixels]}\right) = 0.380 - 0.062\ \log G - 0.092\ (\log G)^2 \tag{3}$$

where G is in electrons. The RMS of the fit is 0.024 pixels. Note that Eq. 3 fits *all* data in the left panel of Figure 5 quite well (i.e., not only the data at the center of the CCD). The right panel of Figure 5 depicts the *evolution* of the centroid shift (at the central location on the CCD) due to CTE effects as a function of time. A comparison with Figure 3 shows that the centroid shifts grow in time with growth rates that are quite similar to those measured for the CTI values themselves. Quantitatively, the data of any given intrinsic signal level shown in Figure 5 can be fit by the function $\mathit{Shift}(t) = \mathit{Shift}(0)\ \times\ [1 + \beta(t - t_0)]$ with β = 0.16 $\pm$ 0.02 and t_0 = 2000.6.

All the above findings indicate that CTE effects cause a fractional loss of signal of which the amplitude is directly related to the size of the associated centroid shift, anywhere on the CCD. This is illustrated in Figure 6, which reveals an extremely tight relation between measured CTI and centroid shift. The solid line depicts the least-square fit to this relation,

$$\text{Centroid Shift [pixels]} = 0.081\ \left(\frac{\text{CTI}}{10^{-4}}\right)\ - 0.002\ \left(\frac{\text{CTI}}{10^{-4}}\right)^2 \tag{4}$$

which has an RMS error of only 0.01 pixels. Eq. 4 should prove useful for science programs for which both accurate spectrophotometry *and* astrometry is important. Note that this relation formally only holds for the (default) gain = 1 setting. Issues related to the gain = 4 setting are discussed next.

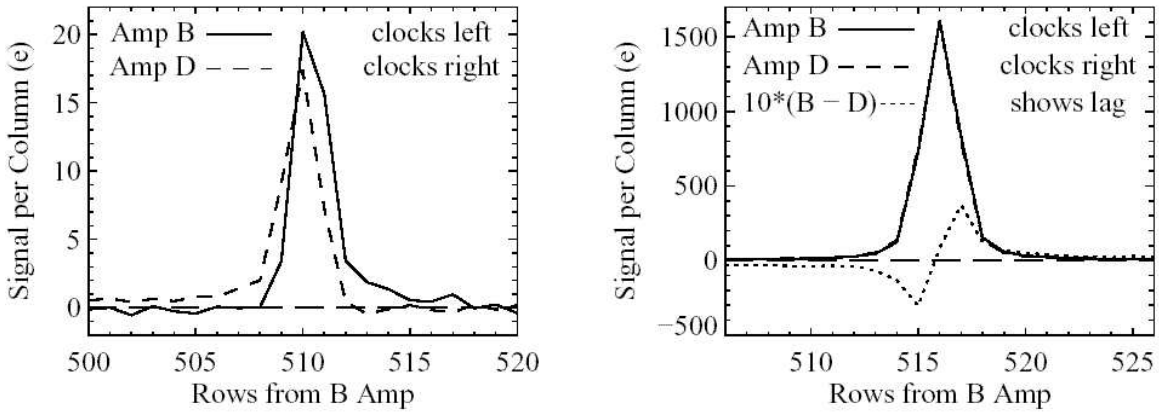

Figure 4: Comparison of line profiles obtained when clocking a given exposure in opposite directions in the internal sparse field test. At low signal levels (left panel), charge trailing and centroid shift are obvious. Even at high signal levels (right panel), differences in the line profile are systematic and measureable (the dotted line depicts the difference profile). Figure reproduced from Kimble, Goudfrooij, & Gilliland (2000).

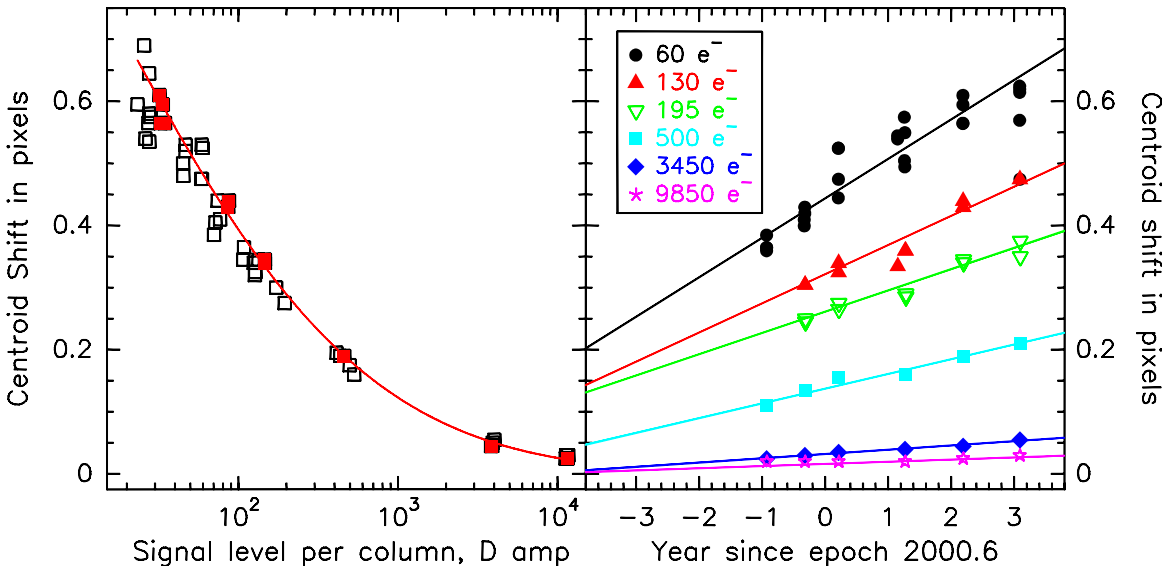

Figure 5: *Left panel*: The centroid shift (in unbinned CCD pixels) as a function of signal level as read out by the D amplifier for the gain = 1 observing block in October 2002, ∼ 5.5 years after STIS installation. Centroid shifts for the central location on the CCD are shown in filled squares, and a least-squares fit to the latter is shown by the solid line. *Right panel*: The centroid shift for the central location on the CCD as functions of time and signal level as read out by the D amplifier. Both the data and the corresponding linear fits are plotted. Symbols associated with individual signal levels (corrected for CTI) are indicated in the legend.

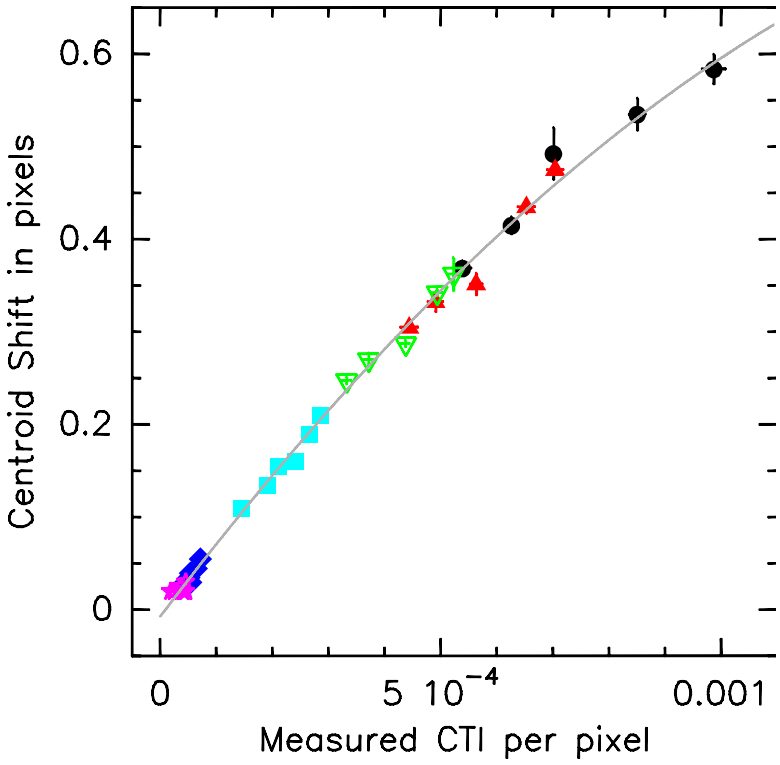

Figure 6: The centroid shift as a function of CTI for all gain = 1 datasets. Symbols as in Figures 3 and 5. Note the very tight relation between the two properties. A least-squares fit to the data (cf. Eq. 4) is shown by the solid line.

3.2 Gain = 4

The gain = 4 e$^-$/DN setting of the STIS CCD has several features which render it useful only for very high signal-to-noise observations. It allows one to reach the full well of the CCD at at the cost of a significantly higher read noise than the gain = 1 setting (see Chapter 7 in Kim Quijano et al. 2004), and it does not sample the sky background level well in typical spectroscopic exposures. With this in mind, the bias voltages for the gain = 4 setting were set by the STIS instrument definition team (during ground testing) with the main goal to obtain the best possible performance at high signal levels.

One (minor) issue associated with this choice of bias voltage for the gain = 4 setting is the high level of spurious charge injected during the readout process of the STIS CCD (see also Goudfrooij & Walsh 1997). The properties of this spurious charge can be measured from the gain = 4 bias files. Its main feature is a steep ramp in the half of the CCD furthest away from the readout amplifier, which has a significant effect on the CTI measurements in this report. This is illustrated in Figure 7, which shows a comparison of the spurious charge levels in gain = 1 vs. gain = 4 and the resulting effect on the CTE-related signal losses as a function of distance from the readout amplifier. Obviously, CTI values derived using "B-amp/D-amp" signal ratios are lower in gain = 4 than in gain = 1. Furthermore, the derived CTI values for gain = 4 contain systematic errors due to the steep ramp of the spurious charge in the bias level, especially for low signal levels where the extra spurious charge for gain = 4 helps a lot in filling charge traps. However, as we are mainly interested in the CTI performance of the gain = 4 setting at high signal levels, this issue is deemed unimportant.

The derived CTI values for gain = 4 are shown in Fig. 8 as a function of time. For comparison, the fits

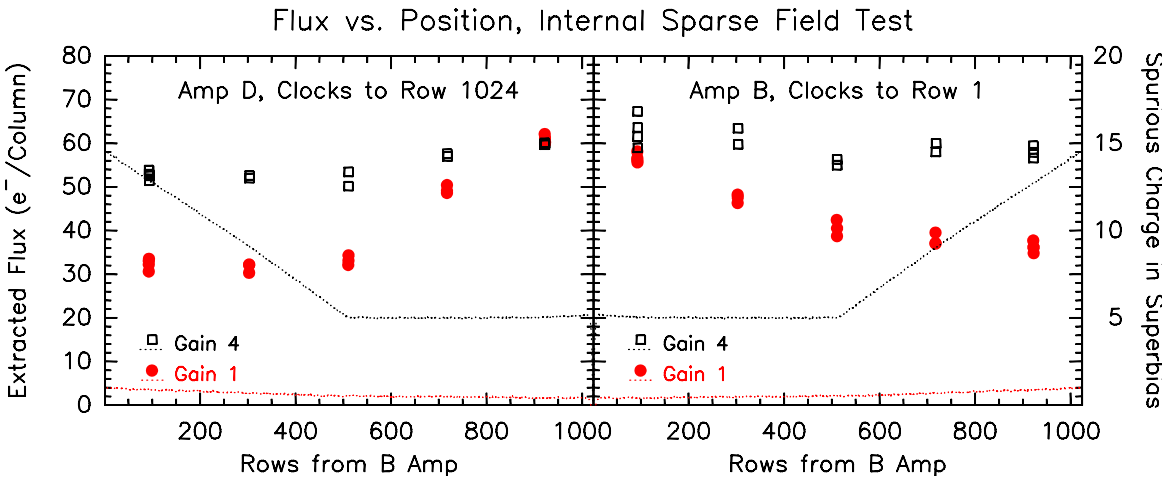

Figure 7: Illustration of the effect of spurious charge in STIS bias frames to the resulting CTI, and a comparison between gain = 1 and gain = 4 data. *Left panel:* The symbols represent extracted signal levels (see left-hand ordinate) as a function of CCD row number for the 60 e^-/column dataset read out using amplifier D and taken during the Fall 2000 observing block. The dotted lines represent the spurious charge level of STIS CCD superbias frames (see right-hand ordinate) as function of row number. Red lines and symbols represent gain = 1 data, while black lines and symbols represent gain = 4 data. *Right panel:* Same as left panel, but for signal levels measured from images read out with amplifier B, located on the serial register opposite to that of amplifier D. Note the strong influence of the steep slope of the spurious charge level in gain = 4 across half the field.

derived from the gain = 1 data are shown as solid lines. The left panel shows the derived with a spurious-charge correction of 5 counts (as in the "flat" part of the gain = 4 bias structure) and the right panel with a correction of 8 counts (half way up the spurious charge ramp). As expected, the data is noisier than for the gain = 1 case and the CTI values for gain = 4 are significantly lower than those of gain = 1 for the low signal levels. However, the gain = 4 results are consistent with the gain = 1 ones at signal levels of ~ 1000 e^- and above, for which the gain = 4 setting was created in the first place. Given the features of the gain = 4 setting mentioned above, we have not derived a CTE degradation time constant α (cf. Eq. 2) separately for gain = 4. I.e., the STIS pipeline CALSTIS performs the CTE correction using the value of α determined from gain = 1 data (Table 3).

References

Bohlin, R. C., & Goudfrooij, P., 2003, STIS Instrument Science Report 2003-03 (Baltimore: STScI)
Gilliland, R. L., Goudfrooij, P., & Kimble, R. A., 1999, PASP, 111, 1009
Goudfrooij, P., & Walsh, J. R., 1997, STIS Instrument Science Report 1997-09 (Baltimore: STScI)
Goudfrooij, P., & Kimble, R. A., 2003, in Proc. 2002 HST Calibration Workshop, ed. S. Arribas, A. Koekemoer, & B. Whitmore (Baltimore: STScI), p. 105
Kim Quijano, J., et al., 2004, STIS Instrument Handbook (Baltimore: STScI)
Kimble, R. A., Goudfrooij, P., & Gilliland, R. L., 2000, Proc. SPIE, 4013, p. 532
Leitherer, C., & Bohlin, R. C., 1997, Instrument Science Report STIS 97-13 (Baltimore: STScI)
McGrath, M. A., Busko, I., & Hodge, P., 1999, STIS Instrument Science Report 1999-03 (Baltimore: STScI)
Riess, A., & Mack, J., 2004, ACS Instrument Science Report 2004-06 (Baltimore: STScI)
Whitmore, B. C., Heyer, I., & Casertano, S., PASP, 111, 1559

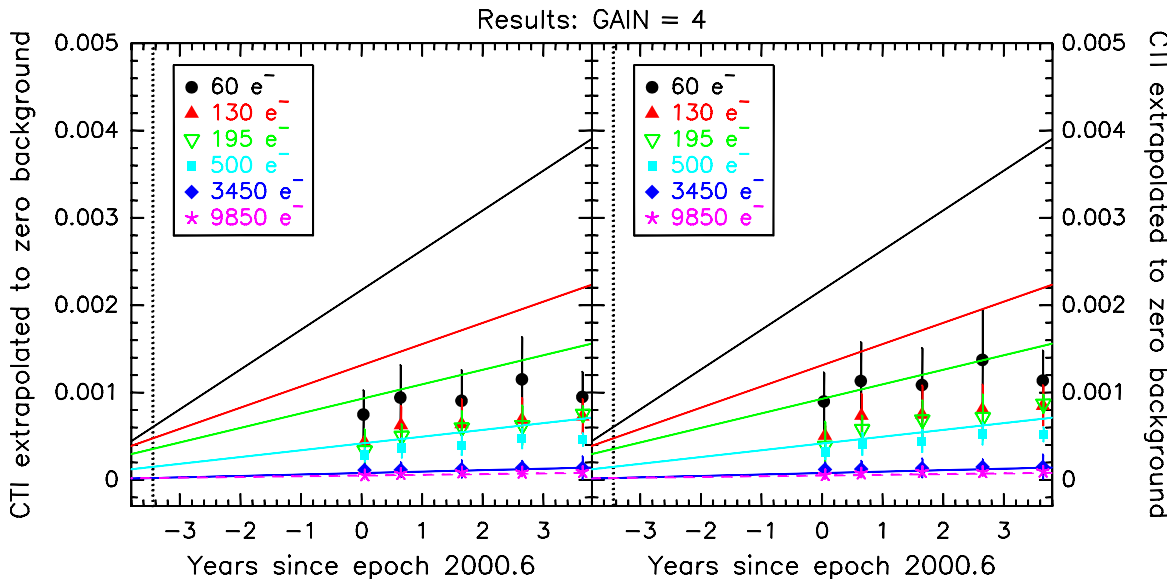

Figure 8: *Left panel:* CTI extrapolated to zero background for gain = 4 as a function of time and signal level, derived from the internal sparse field test. Symbols associated with individual signal levels (corrected for CTI) are indicated in the legend. A spurious charge level of 5 e^- was assumed for the correction to zero background. The linear fits (solid lines) represent the fits to the gain = 1 data (taken from Fig. 3) for the purpose of comparison. It is clear that the derived CTI values for low-signal data are much lower for gain = 4 than for gain = 1. The epoch of HST Servicing Mission 2 (during which STIS was installed on HST) is depicted as a black dotted line. *Right panel:* Same as left panel, except that a spurious charge level of 8 e^- was assumed. See Fig 7 and text in Section 3.2 regarding issues related to spurious charge level in gain = 4.